Autocatalytic-Amplificative Detection of Ethylene

Autumn I. Giger, Jaiden C. Voldrich, and Brian W. Michel*

Department of Chemistry and Biochemistry, University of Denver, Denver, Colorado 80210, United States

Abstract

Amplified sensing systems offer the potential for high sensitivity; however, the vast majority of molecular strategies involve stoichiometric detection and signal transduction, including numerous recent examples of systems inspired by transition metal catalyzed reactions. Allosteric catalysis via activation of latent precatalysts by a target analyte represents an attractive strategy for detecting low concentration species. Analyte amplification represents another attractive approach, akin to PCR-based assays. Here we report the development of an autocatalytic detection system based on ethylene activation of latent Ru-based olefin metathesis precatalysts. Signal transduction is amplified both by catalytic ring closing metathesis of profluorescent substrates and ethylene propagation to activate additional units of latent catalyst. High sensitivity is observed as a result of this dual-mode Amplified Detection of Ethylene (ADE). Detection of endogenous ethylene from fruit and oxidation-decomposition of polyunsaturated fatty acids via lipid peroxides is demonstrated.

Introduction

Molecular sensing is a powerful strategy with a wide range of applications ranging from consumer facing test kits to valuable tools in chemical biology. In addition to product and tool development, a number of novel strategies have evolved from a push to develop increasingly sensitive and selective systems that draw on a variety of techniques in the chemists' toolbox. There are two critical aspects to a molecular sensing system: 1) analyte recognition and 2) signal transduction.[1,2] Analyte recognition can be broadly categorized as Coordination-Based or Activity-Based (i.e. reaction-based).[3] In both categories, signal is either directly or indirectly converted into a readily detected response (e.g. electrochemical, colorimetric, or fluorescence). Most systems involve a stoichiometric analyte recognition and signal transduction process; that is one molecule of analyte is detected and converted to one unit of signal. In contrast, highly sensitive amplified systems exist where one analyte detection event results in multiple units of signal transduction. Many of these examples come from nature, with ELISA and PCR-based systems being the most prominent. These systems catalytically amplify the number of signal transduction- or analyte molecules respectively.[4–7]

In the continual pursuit of nature mimicry, a number of purely synthetic amplified sensing systems have been reported; including catalyst release from Anslyn,[8] analyte catalysis from Kodie,[9] self-immolative

dendrimers pioneered by Shabat,[10–12] and autocatalytic amplifying systems from Phillips[13,14] being exemplary cases. The supramolecular allosteric catalysis systems from Yoon and Mirkin is particularly noteworthy.[15,16] In this system, coordination of acetate ion, under CO atmosphere, induces the catalytic generation of additional acetate and is effectively an autocatalytic means of acetate detection. This is a rare example of a synthetic mimic of a PCR-like amplification and remains one of the only examples despite ~20 years of efforts. The various approaches to amplificative analyte detection and classification of approaches have been reviewed.[17–20]

Given the enumerable advancements enabled by transition metal catalysis, it is not surprising that it has been adopted by a number of the aforementioned amplified sensing systems. Additionally, transition metals-based systems have emerged as novel approaches for the detection of small, relatively unreactive analytes, which are challenging to detect with main group chemistry. Recently developed systems for the detection of carbon monoxide and ethylene are prime examples of such analytes.[21–27] Largely driven by its critical signaling role in plants[28,29] and its potential as a non-invasive biomarker of oxidative stress in mammals,[30–33] our group has been particularly interested in the detection of ethylene. Recently we reported an Activity-Based Sensor (ABS) for ethylene detection based on the reaction of a Hoveyda-Grubbs 2nd generation catalyst complex appended with a fluorophore on the chelating isopropoxy ligand.[22] In this ABS system a reaction occurs following ethylene coordination, effectively the initiation step of catalytic olefin metathesis. Other molecular approaches to ethylene detection have been reported by Burstyn, Swager, Kodera, and others that can be categorized as coordination-based sensors. Here, analyte detection occurs via the coordination of ethylene to a metal center, typically Ag[34–38] or Cu[39–41], with signal transduction via optical, chemiresistive, or gravimetric responses (Fig. 1a).[27] Additional examples of ABS probes for ethylene have been reported since,[42] including strategies employing protein-ABS adducts[43,44] and cyclorhodinated complexes[45]. Additional early examples likely proceed via a stoichiometric Wacker oxidation.[46,47] In another creatively designed Wacker approach, Swager and coworkers reported a system that is catalytic in Pd, although signal transduction remains stoichiometric.[48] While these strategies have been demonstrated in various sensing and biological studies, it seems unfortunate that these innovative adaptations of catalytic transformations provide only stoichiometric signal transduction (Fig. 1b). Given the high sensitivities enabled by molecular amplification strategies, we sought to investigate catalytic approaches for an amplified detection of ethylene (ADE).

When considering how to achieve ADE we thought to decouple ethylene detection from signal transduction. We hypothesized that a sterically encumbered metathesis precatalyst would be inert to essentially all alkenes, yet could still react with the smallest alkene, ethylene, providing a highly reactive Ru-

methylidene ($Ru{=}CH_2$) (Fig. 1c). This reactive species generated *in situ* could then perform catalytic ring closing metathesis (RCM) with an appropriate signal transduction substrate, thereby amplifying the ethylene detection event. Notably, ethylene is a byproduct of metathesis reactions between terminal alkenes. Therefore, ethylene generated from signal transduction concurrently amplifies analyte concentration – inducing activation of additional latent catalyst units. Herein, we describe an approach to ADE via activation of latent olefin metathesis catalysts resulting in a signal output that is amplified by both catalysis and analyte amplification, which can be applied to the detection of ethylene from biologically relevant samples.

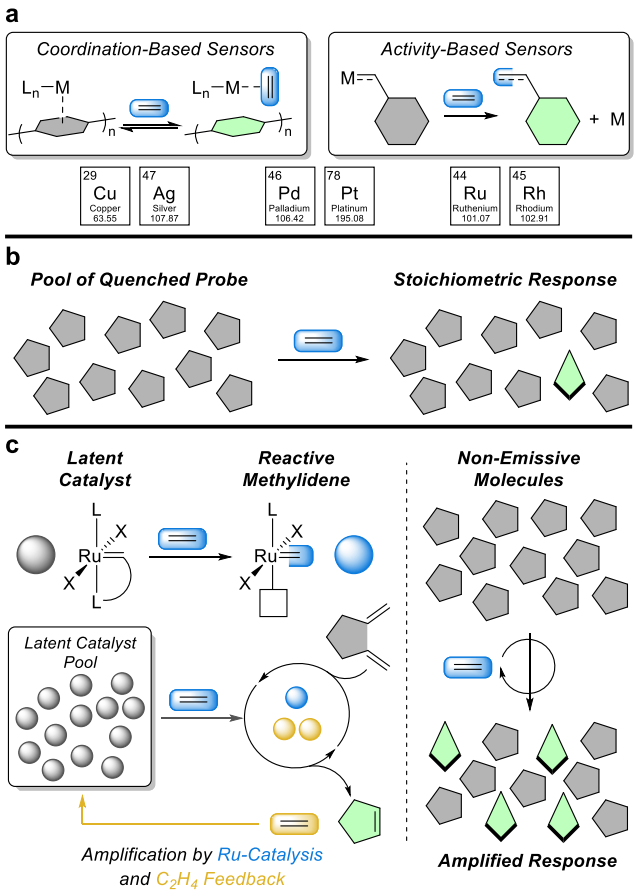

Fig. 1 | Previously reported stoichiometric probes and introduction of proposed system. (a) Overview of concepts used in previous molecular approaches for ethylene detection. **(b)** Conventional stoichiometric signal transduction. **(c)** Concept of amplified detection of ethylene.

Results and Discussion

Validation of Ethylene Autocatalytic Behavior

A critical component of the hypothesized ADE strategy was the identification of a catalyst with high latency for the profluorescent substrates that could be activated by ethylene. The large number of reported metathesis catalysts and possible combinations of ligand modifications makes preliminary catalyst

identification a potentially daunting task. A number of metathesis complexes have been reported to demonstrate latent behavior, although these efforts have largely centered around ring opening metathesis polymerization (ROMP) reactions.[49–52] Further, in the extensive metathesis literature ethylene is often ignored, or viewed as having negative consequences in catalytic RCM; however, numerous examples exist where ethylene has a positive or requisite role.[53–57]

Recently, a number of potentially beneficial effects have been described for metathesis catalysts where the anionic chloride ligands have been replaced with iodides.[58–60] In particular, we were drawn to recent work from Skowerski and coworkers, who reported on the robust nature and selectivity of iodide (I2) complexes.[61] An intriguing result reported in this manuscript describes a lag phase for the sterically encumbered **nG-SIPr-I2**, which is ablated in the presence of ethylene. The authors suggest that the rapid initiation in the presence of ethylene is the result of an initial reaction between the catalysts and ethylene to generate a highly active methylidene species (Fig. 2a). In the absence of added ethylene, a sigmoidal kinetic profile was observed (i.e. lag phase followed by rapid acceleration). To us, this suggests that slow initial reaction of the substrate with the complex produced ethylene as a byproduct, which could react with the sterically encumbered complex again, generating a high activity methylidene catalyst. To validate this hypothesis, we monitored the RCM of TsN(allyl)$_2$ by NMR with varying amounts of ethylene injected into a septum sealed NMR tube. The sigmoidal reaction profiles demonstrate ethylene modulated dose dependence (Fig. 2b). Monitoring dissolved ethylene shows increasing [C_2H_4] over time and clearly correlates with the acceleration of reaction velocity (Fig. S1). These data support the autocatalytic behavior of this system and suggests I2 complexes as a promising class of latent precatalysts that could act as ethylene recognition elements in a sensing system.[62–64]

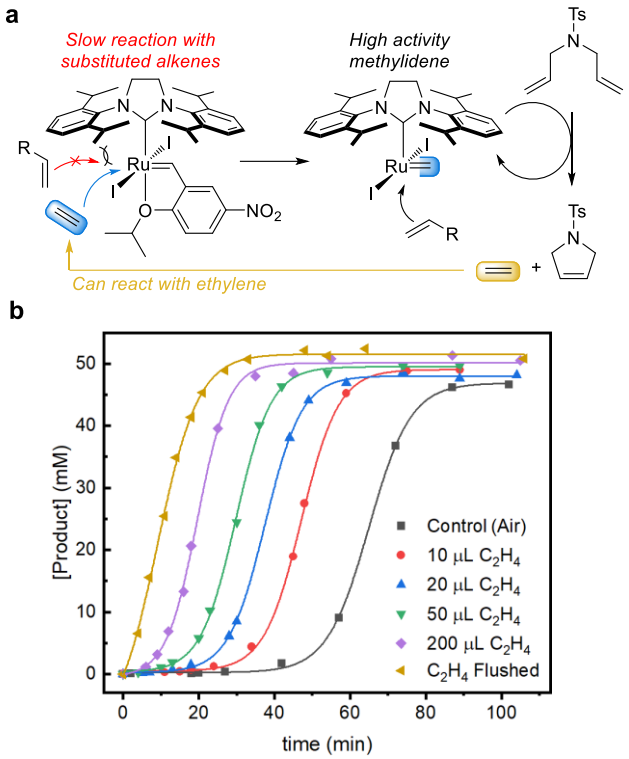

Fig. 2 | Validation of autocatalytic behavior and ethylene modulated autocatalysis. (a) Molecular rational of ethylene activation and autocatalytic behavior. **(b)** Kinetic profiles for the RCM of TsN(allyl)$_2$ monitored by NMR with varying [C_2H_4].

Catalyst and Signal Transduction System

We sought to evaluate a series Ru-I2 complexes along with standard metathesis catalysts, and a select group of other catalysts (Fig. 3a). To achieve optical signal transduction, we favored profluorescent RCM substrates due to the low background signal, which can facilitate high sensitivity. Further, we were inspired by previous reports of profluorescent substrates from the Ward group, which provide products with increased fluorescence either by fluorophore synthesis or cleavage of an appended quencher.[65,66] In our hands, the pro-umbelliferone (**ProU**) substrate was prone to polymerization and/or decomposition, and the methacrylate analogue (**Pro3MU**, R = Me, Fig. 3b) demonstrated increased stability, particularly when stabilized with BHT (~1000 ppm). Additionally, we prepared the dansyl-quencher (**DQ-1**, Fig. 3c) substrate; a slightly modified version of the previously reported substrate.

Following brief optimization, product formation from both substrates was evaluated by monitoring fluorescence intensity over time in the absence of added ethylene or following injection of 20 µL of ethylene gas into septum sealed cuvettes. The less reactive **Pro3MU** substrate was evaluated in toluene at 50 °C (Fig 3d). Under these conditions, Ru-I2 complexes bearing saturated imidazole NHC ligands were the most promising. Little to no fluorescence response was observed in the absence of ethylene with a strong

response after exposed to ethylene. CAAC-I2 complexes were relatively slow to react or inert under the employed conditions; other I2 complexes were unimpressive; and it is not surprising that phosphine containing complexes (e.g. **G1**, **G2**) performed worse in the presence of ethylene. Similar patterns of catalyst reactivity were observed for **DQ-1** at room temperature, although with notably faster product formation at lower substrate and catalyst concentrations (Fig. 3e).

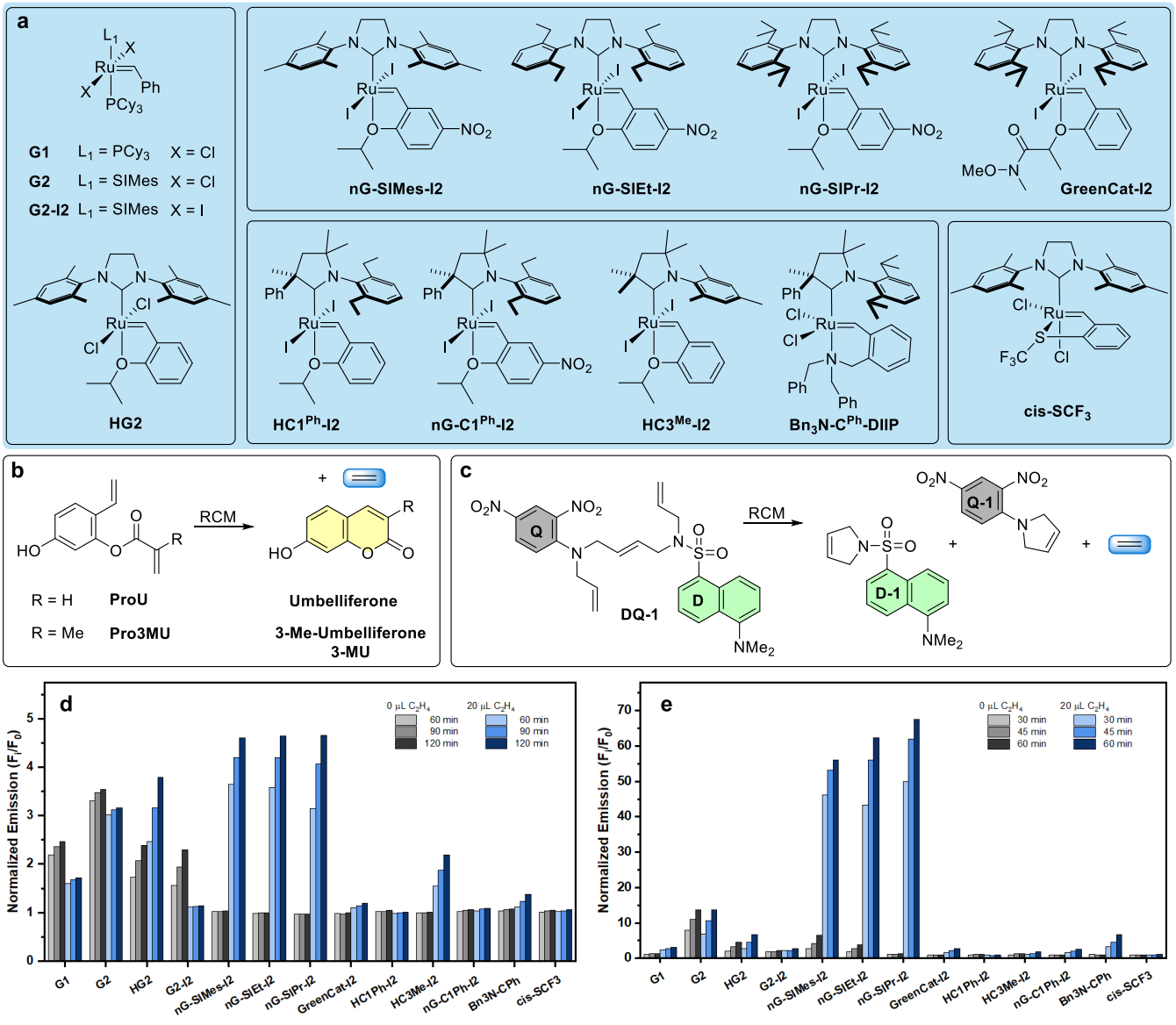

Fig. 3 | Catalyst latency and activation experiments with Pro3MU and DQ-1 substrates. (a) Catalysts evaluated in initial screens. **(b) ProU** and **Pro3MU** undergo RCM to provide umbelliferone and 3-Me-umbelliferone (**3-MU**) as fluorescent products along with ethylene. **(c) DQ-1** and products upon relay RCM. **(d)** Fluorescence catalyst screening results – [**Pro3MU**] = 200 μM, [Catalyst] = 50 μM, PhMe, 50 °C, control (gray), 20 μL C_2H_4 (blue) at 60, 90, 120 min. **(e)** Fluorescence catalyst screening results – [**DQ-1**] = 80 μM, [Catalyst] = 40 μM, PhMe, RT, control (gray), 20 μL C_2H_4 (blue) at 30, 45, 60 min. Details of fluorescence parameters are provided in the supplementary information.

The disparity in latency and rate of signal production is readily rationalized by steric hinderance proximal to the alkene. This is highlighted by monitoring fluorescence increase over time for the two substrates at the same concentration (Fig. 4a). Here **DQ-1**, (30 °C) reaches ~75% of turn-on within just 15 minutes, while **Pro3MU** (50 °C) requires 3 h to reach ~50% turn-on. The tradeoff for faster kinetics of **DQ-1** appears to be a lower degree of latency. Even in the absence of added ethylene, an increase in fluorescence is eventually observed, which supports the autocatalytic nature of this system (Fig. 4b). Slow background reactivity generates ethylene, which is then capable of converting more of the latent catalyst pool into the reactive methylidene. Sufficient latency of **DQ-1** could be obtained with **nG-SIPr-I2** by holding the cuvette temperature at 20 °C, while maintaining robust response to 20 µL ethylene. Higher temperatures resulted in significant catalyst initiation in the absence of ethylene.

Closer examination of **Pro3MU** with the promising I2 complexes (**nG-SIMes-I2**, **nG-SIEt-I2**, and **nG-SIPr-I2**) over time indicated extended latency of all three complexes at 50 °C (Fig. 4c). However, **nG-SIPr-I2** had essentially no fluorescence increase over this time, and for another 180 min, contrasting directly to the modest fluorescence response observed for the **nG-SIMes-I2** and **nG-SIEt-I2** complexes. Injection of 50 µL of ethylene at 180 min resulted in a large fluorescence increase for all three complexes. The lesser turn-on of **nG-SIMes-I2** under these conditions could indicate decomposition of the precatalyst, ethylene adducts, or a greater propensity for unproductive ethylene self-metathesis for more sterically accessible complex. Overall, the limited latency of **DQ-1** and the autocatalytic nature of the system resulted in less consistent control runs. Therefore, the **Pro3MU** substrate was selected for subsequent ADE experiments owing to its robust latency with **nG-SIPr-I2**.

The **Pro3MU**–**nG-SIPr-I2** ADE system shows high selectivity for ethylene (Fig. 4d). Encumbered alkenes (*Z*-disubstituted, 1,1-disubstituted, and trisubstituted) showed no ability to initiate the catalyst system. A very limited response was observed with some small terminal alkenes; however, the response was over an order of magnitude less as compared to ethylene. It is also noteworthy that amplified response was not observed from other substrates, resulting in an increasing magnitude of ethylene selectivity over time.

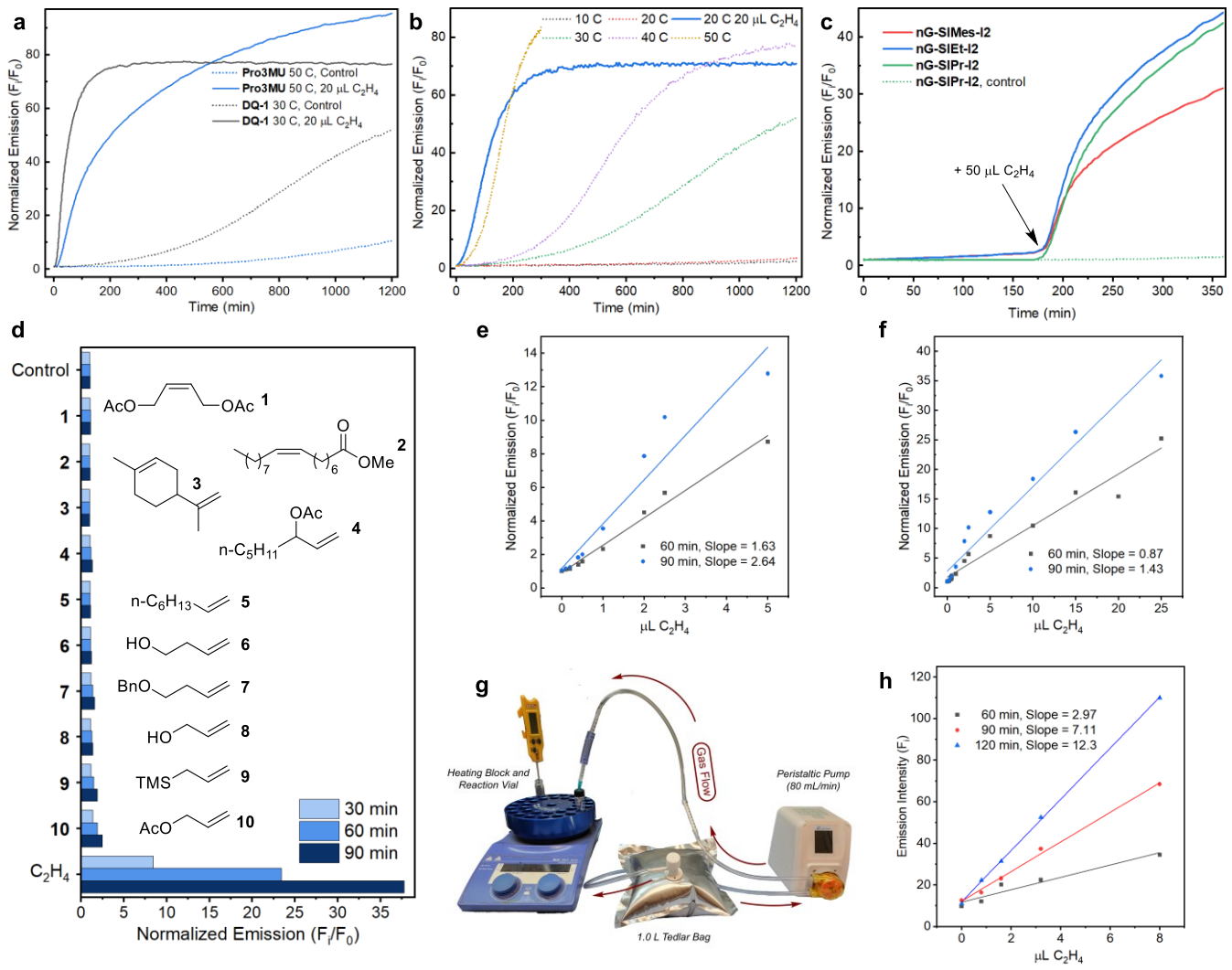

Fig. 4 | Experiments with ethylene gas. (a) Comparison of relative substrate response over time – [**Pro3MU**] = [**DQ-1**] = 100 µM, [**nG-SIPr-I2**] = 50 µM, PhMe; T = 50 °C for **Pro3MU**, T = 30 °C for **DQ-1**. **(b)** Influence of temperature on **DQ-1** latency. [**DQ-1**] = 100 µM, [**nG-SIPr-I2**] = 50 µM. **(c)** Evaluation of extended **Pro3MU** latency with Ru-I2 catalysts. [**Pro3MU**] = 200 µM, [Catalyst] = 50 µM, PhMe, 50 °C, 20 µL C_2H_4 added after 180 min (except control). **(d)** Evaluation of selectivity for C_2H_4 compared to other substrates [**Pro3MU**] = 200 µM, [**nG-SIPr-I2**] = 50 µM, PhMe, 50 °C, [alkenes] = 200 µM or 20 µL C_2H_4 **(e-f)** ADE response of **Pro3MU** to varied C_2H_4 injected into septum sealed cuvettes – [**Pro3MU**] = 200 µM, [**nG-SIPr-I2**] = 50 µM, PhMe, 50 °C. **(g)** Picture and diagram of flow sampling setup. **(h)** Bulk ethylene sampling at low concentrations – Low concentration ethylene samples bubbled through ADE solution of catalyst and substrate [**Pro3MU**] = 200 µM, [**nG-SIPr-I2**] = 50 µM, PhMe, 50 °C. Details of fluorescence parameters are provided in the supplementary information. For panels **e**-**f**, data points represent the mean of 1-5 technical replicates with the exception of control samples (n = 39 technical replicates). For panel **h**, data represents the mean of 3 technical replicates.

Detection of Added Ethylene

The combination of latency with ethylene triggered autocatalysis results in a remarkably sensitive system. As an initial assessment of sensitivity, septum sealed cuvettes containing the ADE reaction mixture were injected with ethylene or ethylene-nitrogen gas mixtures. Due to the small volumes of gas being injected, it is useful to consider the amount (volume or moles) of ethylene detected rather than concentration. An obvious and significant response was observed well below 500 nL (~17 nmol) of injected ethylene (Fig. 4e-f). Two regions of quasi-linearity are observed, the origins of which are not immediately apparent; however, the multifactorial kinetics of this system, increased unproductive ethylene self-metathesis at higher analyte concentrations, and challenges associated with accurately dosing small gas volumes are all plausible explanations. Regardless, considering the low concentration linear range results, LODs are calculated ($3\sigma/k$) to be 58 and 41 nL, or 2.0 and 1.4 nmol, of ethylene at 60 and 90 minutes respectively.

In practice, detection of ethylene in bulk gas samples are of significantly greater total volume. For example, we measured a commercial handheld electrochemical ethylene sensor flowing at 300 mL/min. To better sample dilute ethylene gas mixtures, a flow assay was developed (Fig. 4g). A peristaltic pump operating at 80 mL/min was used to percolate gas samples through a reaction mixture for 2 min, followed by a set time for catalysis before fluorescence measurements were acquired. In these experiments a significant response relative to breathing air was observed into the nL range of total ethylene passed through the system (Fig. 4h). This is well below the sensitivity needed to detect ethylene from plant samples and into the range reported in for ethylene in exhaled breath from mammals.

Validation of Ethylene Detection

As an initial demonstration of the utility, we observed ethylene from apple slices. In plants, 1-aminocyclopropane-1-carboxylic acid (**ACC**) is converted to ethylene by ACC oxidase (**ACO**) (Fig. 5a). Using the flow assay for apple slices sealed in modified glass jars (Fig. S14), basal ethylene levels are readily detected relative to breathing air (Fig. 5b). As an aside, ethylene production from untreated apples varied from day-to-day, due to the natural ripening process; demonstrated by the variable response of apple control samples (Fig. 5b-c). Ethylene production was readily elevated in a dose dependent manner by exogenous addition of **ACC**. To further demonstrate basal ethylene production, we sought to inhibit **ACO** with the known inhibitor pyrazinamide (**PZA**).[67] Apple slices were pretreated with **PZA** resulting in almost complete inhibition of ethylene production, providing an ADE signal near that of the breathing air controls (Fig. 5c). **PZA** pretreatment was effective even when apple slices were later treated with 1 mM **ACC**.

In addition to ethylene's role as a plant hormone, it has been implicated as a biomarker of oxidative stress in mammalian systems arising from lipid peroxides (Fig. 5d).[68,30–33] Weak C–H bonds of polyunsaturated fatty acids (PUFAs), such as linoleic acid, undergo autoxidation to lipid peroxides. Subsequent Fenton-like chemistry and radical fragmentation results in ethylene amongst other products.[69] To assess the potential of ADE from lipid peroxide decomposition, fatty acids were subjected to previously reported conditions that resulted in ethylene production.[30] The headspace was sampled with a modified closed-loop system to account for the reduced sample volume and maximize ethylene dissolution in the ADE reaction mixture (Fig. S15). As expected, stearic acid and oleic acid, saturated and monounsaturated fatty acids respectively, showed no response relative to breathing air or a blank sample with no fatty acid present (Fig. 5e-f). Samples containing the PUFA linoleic acid gave a large ADE response, indicative of ethylene generation. Interestingly, samples of α-linolenic acid suggested lower levels of ethylene production, although the response was still large relative to samples where ethylene was not expected. Possibly, the fewer potential ethylene units in an omega-3 vs an omega-6 PUFA results in less ethylene despite the more facile oxidation of α-linolenic acid. Responses observed for linoleic acid and α-linolenic samples were of similar magnitude to a vial flushed with 100 ppm ethylene gas (~2 nL C_2H_4 in a 20 mL vial). Considering lipid peroxides and excess free iron are hallmarks of ferroptosis, it is likely that ethylene is formed during this important form of programed cell death.[70,71]

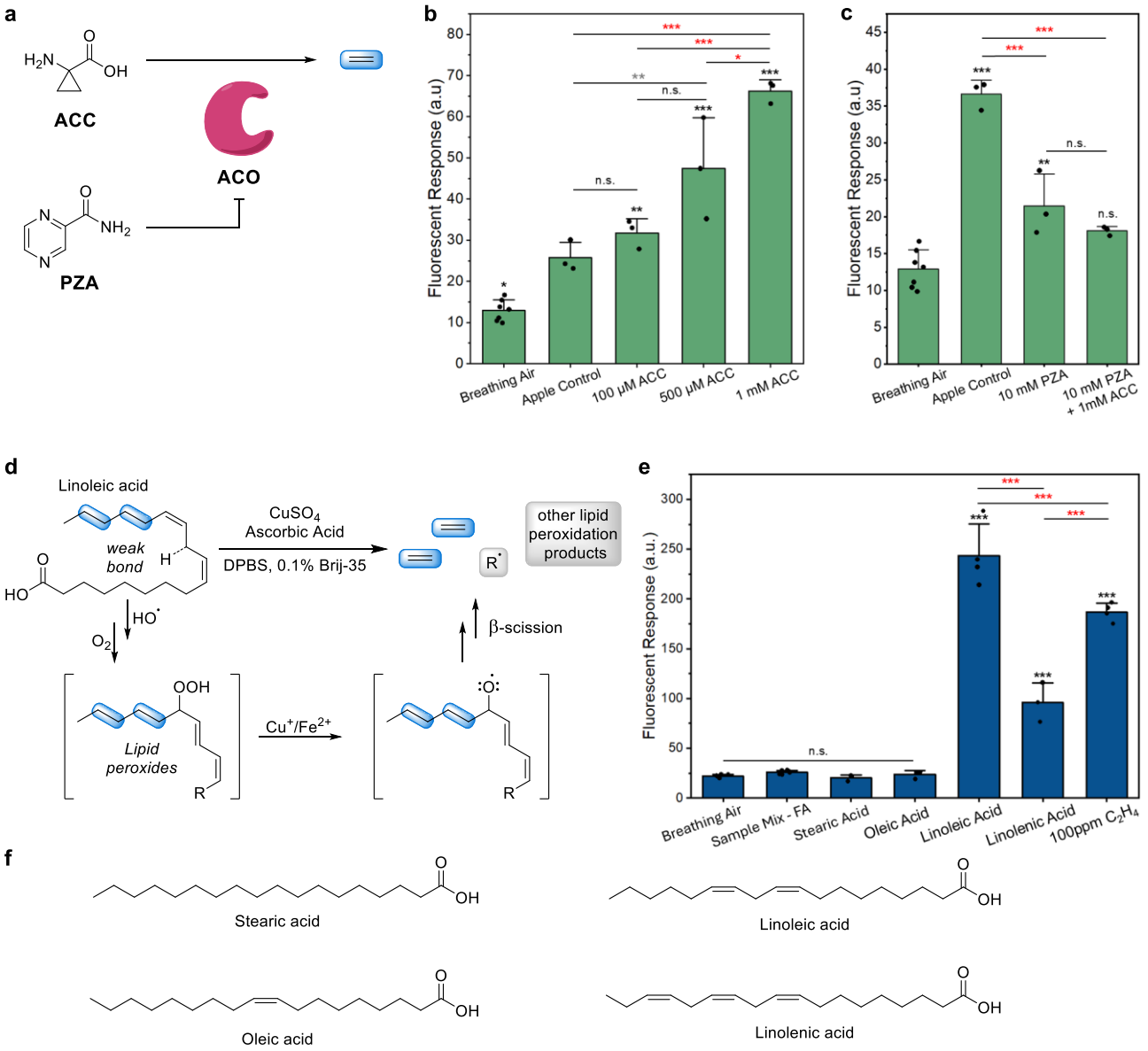

Fig. 5 | ADE sample studies with Pro3MU substrate. (a) Endogenous ethylene precursor **ACC** is converted to ethylene by **ACO**. Known **ACO** inhibitor – **PZA**. **(b)** Basal ethylene production from apple slices and dose dependent increase in ethylene production upon treatment with **ACC**. ADE Conditions: [**Pro3MU**] = 200 µM, [**nG-SIPr-I$_2$**] = 50 µM, PhMe, 50 °C. **(c)** Inhibition of **ACO** by **PZA**. Conditions: [**Pro3MU**] = 200 µM, [**nG-SIPr-I$_2$**] = 50 µM, PhMe, 50 °C. **(d)** Oxidation of linoleic acid to lipid peroxide. Fenton-like chemistry generates ethylene and constituent products. **(e)** ADE response to headspace sampling from peroxidation sample mixtures. Oxidation-fragmentation conditions: 20 mg fatty acid, 0.5 mL 20 mM ascorbic acid, and 0.5 mL 10 mM $CuSO_4$ in 0.1% Brij-35/Dulbecco's PBS. ADE Conditions: [**Pro3MU**] = 200 µM, [**nG-SIPr-I$_2$**] = 50 µM, PhMe, 50 °C. **(f)** Fatty acids used in peroxidation sample mixtures. Scan Parameters for panels **b**, **c**, and **e**: $\lambda_{ex.}$ = 320 nm, λ_{em} = 388-393 nm, Ex. Slit width = 10 nm, Em. Slit width = 10 nm. Data represents a minimum of 3 technical replicates and is reported as the mean ± standard deviation. Data sets were analyzed via one-way ANOVA (two-tailed, unpaired) * $p < 0.05$, ** $p < 0.01$, *** $p < 0.001$, n.s., not statistically significant.

Conclusions

We have developed an analyte triggered amplificative signal transduction system for the detection of ethylene via activation of latent Ru-I2 metathesis precatalysts. The resulting ADE system is highly sensitive and capable of demonstrating significant response from apples at basal, **ACC** supplemented, and **PZA** inhibited levels. Additionally, ethylene was detected from the autoxidation of PUFAs and significant differences were observed between omega-3 and omega-6 PUFAs. A particularly unique aspect of ADE is that two modes of amplification are utilized: 1) Signal Amplification - each catalytic turnover following an initial activation event amplifies response by a factor of the turnover number; and 2) Analyte Amplification - each RCM event propagates an additional equivalent of ethylene, which can activate more of the latent catalyst pool. Specifically, this second process represents autocatalysis – Ru-methylidene generates more Ru-methylidene by way of an ethylene feedback loop.[64] Although this process has been alluded to in the metathesis literature, and induction periods can be observed in many kinetic profiles of RCM reactions, this process is likely specific to certain metathesis precatalysts. To the best of our knowledge this is the first fully synthetic autocatalytic-amplificative system capable of analyte detection from biologically relevant samples. We are currently evaluating approaches to improve and expand this system through catalyst-substrate optimization, sampling improvements, and direct detection of ethylene in models of oxidative stress.

Supplementary Information

Details of experimental procedures and associated data are provided in the Supplementary Information file.

Author Information

Corresponding Author

*Brian W. Michel – Department of Chemistry and Biochemistry, University of Denver, Denver, Colorado 80210, United States. ORCID https://orcid.org/0000-0002-4737-8196; Email: Brian.Michel@du.edu

Authors

Autumn I. Giger – Department of Chemistry and Biochemistry, University of Denver, Denver, Colorado 80210, United States. ORCID https://orcid.org/0009-0007-0032-0097

Jaiden C. Voldrich – Department of Chemistry and Biochemistry, University of Denver, Denver, Colorado 80210, United States. https://orcid.org/0009-0000-8143-6196

Contributions

B.W.M. and A.I.G. conceived and designed the study. A.I.G., J.C.V., and B.W.M. contributed to the synthesis of the substrates and products. A.I.G., J.C.V., and B.W.M. conducted catalytic and time course assays. A.I.G.

and B.W.M. designed and optimized the flow assays. B.W.M. and A.I.G. prepared the manuscript. All authors have given approval to the final version of this manuscript.

Notes

The University of Denver has submitted U.S. Provisional Patent Application Serial # 63/683,597, which covers various aspects of the amplificative ethylene detection technology disclosed in this manuscript. This pending application names Brian Michel, Brady Worrell, Autumn Giger, and Jaiden Voldrich as inventors.

Acknowledgement

Research reported in this publication was supported by the NIGMS National Institute of General Medical Sciences of the National Institutes of Health under Award Number R35GM150937. This work is supported by the USDA National Institute of Food and Agriculture, AFRI project 2022-09139. Purchase of the Avance NEO 600 MHz NMR spectrometer used to obtain results included in this publication was supported by the National Science Foundation under Grant No. DBI 2320158. Christian Blanco (University of Ottawa) and Deryn Fogg (University of Ottawa, University of Bergen) are thanked for samples of catalysts. Apeiron is thanked for gifts of catalysts.

References

(1) You, L.; Zha, D.; Anslyn, E. V. Recent Advances in Supramolecular Analytical Chemistry Using Optical Sensing. *Chem. Rev.* **2015**, *115* (15), 7840–7892. https://doi.org/10.1021/cr5005524.

(2) Grover, K.; Koblova, A.; Pezacki, A. T.; Chang, C. J.; New, E. J. Small-Molecule Fluorescent Probes for Binding- and Activity-Based Sensing of Redox-Active Biological Metals. *Chem. Rev.* **2024**, *124* (9), 5846–5929. https://doi.org/10.1021/acs.chemrev.3c00819.

(3) Bruemmer, K. J.; Crossley, S. W. M.; Chang, C. J. Activity-Based Sensing: A Synthetic Methods Approach for Selective Molecular Imaging and Beyond. *Angew. Chem. Int. Ed.* **2020**, *59* (33), 13734–13762. https://doi.org/10.1002/anie.201909690.

(4) Engvall, E.; Perlmann, P. Enzyme-Linked Immunosorbent Assay (ELISA) Quantitative Assay of Immunoglobulin G. *Immunochemistry* **1971**, *8* (9), 871–874. https://doi.org/10.1016/0019-2791(71)90454-X.

(5) Van Weemen, B. K.; Schuurs, A. H. W. M. Immunoassay Using Antigen—Enzyme Conjugates. *FEBS Letters* **1971**, *15* (3), 232–236. https://doi.org/10.1016/0014-5793(71)80319-8.

(6) Saiki, R. K.; Scharf, S.; Faloona, F.; Mullis, K. B.; Horn, G. T.; Erlich, H. A.; Arnheim, N. Enzymatic Amplification of β-Globin Genomic Sequences and Restriction Site Analysis for Diagnosis of Sickle Cell Anemia. *Science* **1985**, *230* (4732), 1350–1354. https://doi.org/10.1126/science.2999980.

(7) Sano, T.; Smith, C. L.; Cantor, C. R. Immuno-PCR: Very Sensitive Antigen Detection by Means of Specific Antibody-DNA Conjugates. *Science* **1992**, *258* (5079), 120–122. https://doi.org/10.1126/science.1439758.

(8) Wu, Q.; Anslyn, E. V. Catalytic Signal Amplification Using a Heck Reaction. An Example in the Fluorescence Sensing of Cu(II). *J. Am. Chem. Soc.* **2004**, *126* (45), 14682–14683. https://doi.org/10.1021/ja0401038.

(9) Song, F.; Garner, A. L.; Koide, K. A Highly Sensitive Fluorescent Sensor for Palladium Based on the Allylic Oxidative Insertion Mechanism. *J. Am. Chem. Soc.* **2007**, *129* (41), 12354–12355. https://doi.org/10.1021/ja073910q.

(10) Amir, R. J.; Pessah, N.; Shamis, M.; Shabat, D. Self-Immolative Dendrimers. *Angewandte Chemie International Edition* **2003**, *42* (37), 4494–4499. https://doi.org/10.1002/anie.200351962.

(11) Sella, E.; Shabat, D. Dendritic Chain Reaction. *J. Am. Chem. Soc.* **2009**, *131* (29), 9934–9936. https://doi.org/10.1021/ja903032t.
(12) Sella, E.; Lubelski, A.; Klafter, J.; Shabat, D. Two-Component Dendritic Chain Reactions: Experiment and Theory. *J. Am. Chem. Soc.* **2010**, *132* (11), 3945–3952. https://doi.org/10.1021/ja910839n.
(13) Baker, M. S.; Phillips, S. T. A Two-Component Small Molecule System for Activity-Based Detection and Signal Amplification: Application to the Visual Detection of Threshold Levels of Pd(II). *J. Am. Chem. Soc.* **2011**, *133* (14), 5170–5173. https://doi.org/10.1021/ja108347d.
(14) Mohapatra, H.; Schmid, K. M.; Phillips, S. T. Design of Small Molecule Reagents That Enable Signal Amplification via an Autocatalytic, Base-Mediated Cascade Elimination Reaction. *Chem. Commun.* **2012**, *48* (24), 3018–3020. https://doi.org/10.1039/C2CC17566E.
(15) Gianneschi, N. C.; Nguyen, S. T.; Mirkin, C. A. Signal Amplification and Detection via a Supramolecular Allosteric Catalyst. *J. Am. Chem. Soc.* **2005**, *127* (6), 1644–1645. https://doi.org/10.1021/ja0437306.
(16) Yoon, H. J.; Mirkin, C. A. PCR-like Cascade Reactions in the Context of an Allosteric Enzyme Mimic. *J. Am. Chem. Soc.* **2008**, *130* (35), 11590–11591. https://doi.org/10.1021/ja804076q.
(17) Scrimin, P.; Prins, L. J. Sensing through Signal Amplification. *Chem. Soc. Rev.* **2011**, *40* (9), 4488–4505. https://doi.org/10.1039/C1CS15024C.
(18) Goggins, S.; Frost, C. G. Approaches towards Molecular Amplification for Sensing. *Analyst* **2016**, *141* (11), 3157–3218. https://doi.org/10.1039/C6AN00348F.
(19) Sun, X.; Shabat, D.; Phillips, S. T.; Anslyn, E. V. Self-Propagating Amplification Reactions for Molecular Detection and Signal Amplification: Advantages, Pitfalls, and Challenges. *Journal of Physical Organic Chemistry* **2018**, *31* (8), e3827. https://doi.org/10.1002/poc.3827.
(20) Choudhury, A. R.; Dey, N. Molecular Amplification as an Affordable Strategy for Trace-Level Detection of Ionic Analytes with Fluorimetric or Colorimetric Readout. *ChemPhotoChem* **2023**, *7* (6), e202200306. https://doi.org/10.1002/cptc.202200306.
(21) Michel, B. W.; Lippert, A. R.; Chang, C. J. A Reaction-Based Fluorescent Probe for Selective Imaging of Carbon Monoxide in Living Cells Using a Palladium-Mediated Carbonylation. *J. Am. Chem. Soc.* **2012**, *134* (38), 15668–15671.
(22) Toussaint, S. N. W.; Calkins, R. T.; Lee, S.; Michel, B. W. Olefin Metathesis-Based Fluorescent Probes for the Selective Detection of Ethylene in Live Cells. *J. Am. Chem. Soc.* **2018**, *140* (41), 13151–13155. https://doi.org/10.1021/jacs.8b05191.
(23) Crossley, S. W. M.; Tenney, L.; Pham, V. N.; Xie, X.; Zhao, M. W.; Chang, C. J. A Transfer Hydrogenation Approach to Activity-Based Sensing of Formate in Living Cells. *J. Am. Chem. Soc.* **2024**, *146* (13), 8865–8876. https://doi.org/10.1021/jacs.3c09735.
(24) Strianese, M.; Pellecchia, C. Metal Complexes as Fluorescent Probes for Sensing Biologically Relevant Gas Molecules. *Coord. Chem. Rev.* **2016**, *318*, 16–28. https://doi.org/10.1016/j.ccr.2016.04.006.
(25) Ohata, J.; Bruemmer, K. J.; Chang, C. J. Activity-Based Sensing Methods for Monitoring the Reactive Carbon Species Carbon Monoxide and Formaldehyde in Living Systems. *Acc. Chem. Res.* **2019**, *52* (10), 2841–2848. https://doi.org/10.1021/acs.accounts.9b00386.
(26) Walvoord, R. R. ; Schneider, M. R. ;; Michel, B. W. Fluorescent Probes for Intracellular Carbon Monoxide Detection. In *Carbon Monoxide in Drug Discovery: Basics, Pharmacology, and Therapeutic Potential*; Wang, B. and O., Ed.; John Wiley & Sons: Hoboken, NJ, 2022; pp 321–344.
(27) Jensen, K. H.; Michel, B. W. Detection of Ethylene with Defined Metal Complexes: Strategies and Recent Advances. *Analysis & Sensing* **2023**, *3* (2), e202200058. https://doi.org/10.1002/anse.202200058.
(28) Alonso, J. M.; Stepanova, A. N. The ethylene signaling pathway. *Science (Washington, DC, U. S.)* **2004**, *306* (5701), 1513–1515.

(29) Fernandez-Moreno, J.-P.; Stepanova, A. N. Monitoring Ethylene in Plants: Genetically Encoded Reporters and Biosensors. *Small Methods* **2020**, *4* (8), 1900260. https://doi.org/10.1002/smtd.201900260.
(30) Dumelin, E. E.; Tappel, A. L. Hydrocarbon Gases Produced during in Vitro Peroxidation of Polyunsaturated Fatty Acids and Decomposition of Preformed Hydroperoxides. *Lipids* **1977**, *12* (11), 894. https://doi.org/10.1007/BF02533308.
(31) Harren, F. J. M.; Berkelmans, R.; Kuiper, K.; te Lintel Hekkert, S.; Scheepers, P.; Dekhuijzen, R.; Hollander, P.; Parker, D. H. On-Line Laser Photoacoustic Detection of Ethene in Exhaled Air as Biomarker of Ultraviolet Radiation Damage of the Human Skin. *Appl. Phys. Lett.* **1999**, *74* (12), 1761–1763. https://doi.org/10.1063/1.123680.
(32) Cristescu, S. M.; Kiss, R.; te Lintel Hekkert, S.; Dalby, M.; Harren, F. J. M.; Risby, T. H.; Marczin, N. Real-Time Monitoring of Endogenous Lipid Peroxidation by Exhaled Ethylene in Patients Undergoing Cardiac Surgery. *American Journal of Physiology-Lung Cellular and Molecular Physiology* **2014**, *307* (7), L509–L515. https://doi.org/10.1152/ajplung.00168.2014.
(33) Paardekooper, L. M.; van den Bogaart, G.; Kox, M.; Dingjan, I.; Neerincx, A. H.; Bendix, M. B.; Beest, M. ter; Harren, F. J. M.; Risby, T.; Pickkers, P.; Marczin, N.; Cristescu, S. M. Ethylene, an Early Marker of Systemic Inflammation in Humans. *Sci. Rep.* **2017**, *7* (1), 6889. https://doi.org/10.1038/s41598-017-05930-9.
(34) Green, O.; Smith, N. A.; Ellis, A. B.; Burstyn, J. N. AgBF4-Impregnated Poly(vinyl phenyl ketone): An Ethylene Sensing Film. *J. Am. Chem. Soc.* **2004**, *126* (19), 5952–5953.
(35) Santiago Cintrón, M.; Green, O.; Burstyn, J. N. Ethylene Sensing by Silver(I) Salt-Impregnated Luminescent Films. *Inorg. Chem.* **2012**, *51* (5), 2737–2746. https://doi.org/10.1021/ic102590f.
(36) Hitomi, Y.; Nagai, T.; Kodera, M. A silver complex with an N,S,S-macrocyclic ligand bearing an anthracene pendant arm for optical ethylene monitoring. *Chem. Commun. (Cambridge, U. K.)* **2012**, *48* (84), 10392–10394.
(37) Marti, A. M.; Nijem, N.; Chabal, Y. J.; Balkus, K. J. Selective Detection of Olefins Using a Luminescent Silver-Functionalized Metal Organic Framework, RPM3. *Microporous Mesoporous Mater.* **2013**, *174*, 100–107. https://doi.org/10.1016/j.micromeso.2013.02.044.
(38) Tolentino, M. A. K. P.; Albano, D. R. B.; Sevilla, F. B. Piezoelectric Sensor for Ethylene Based on Silver(I)/Polymer Composite. *Sensors and Actuators B: Chemical* **2018**, *254*, 299–306. https://doi.org/10.1016/j.snb.2017.07.015.
(39) Esser, B.; Swager, T. M. Detection of ethylene gas by fluorescence turn-on of a conjugated polymer. *Angew. Chem. Int. Ed.* **2010**, *49* (47), 8872–8875, S8872/1-S8872/15.
(40) Esser, B.; Schnorr, J. M.; Swager, T. M. Selective detection of ethylene gas using carbon nanotube-based devices: Utility in determination of fruit ripeness. *Angew. Chem. Int. Ed.* **2012**, *51* (23), 5752–5756, S5752/1-S5752/13.
(41) Fu, W.; van Dijkman, T. F.; Lima, L. M. C.; Jiang, F.; Schneider, G. F.; Bouwman, E. Ultrasensitive Ethene Detector Based on a Graphene–Copper(I) Hybrid Material. *Nano Lett.* **2017**, *17* (12), 7980–7988. https://doi.org/10.1021/acs.nanolett.7b04466.
(42) Sun, M.; Yang, X.; Zhang, Y.; Wang, S.; Wong, M. W.; Ni, R.; Huang, D. Rapid and Visual Detection and Quantitation of Ethylene Released from Ripening Fruits: The New Use of Grubbs Catalyst. *J. Agric. Food. Chem.* **2019**, *67* (1), 507–513. https://doi.org/10.1021/acs.jafc.8b05874.
(43) Vong, K.; Eda, S.; Kadota, Y.; Nasibullin, I.; Wakatake, T.; Yokoshima, S.; Shirasu, K.; Tanaka, K. An Artificial Metalloenzyme Biosensor Can Detect Ethylene Gas in Fruits and Arabidopsis Leaves. *Nature Communications* **2019**, *10* (1), 5746. https://doi.org/10.1038/s41467-019-13758-2.
(44) Wu, M.; Yin, C.; Fu, L.; Liu, T.; Jiang, M.; Sun, Q.; Chen, L.; Niu, N. A Biocompatible Ruthenium-Based Composite Fluorescent Probe Using Bovine Serum Albumin as a Scaffold for Ethylene Gas Detection

and Its Fluorescence Imaging in Plant Tissues. *Chem. Eng. J.* **2022**, *435*, 135045. https://doi.org/10.1016/j.cej.2022.135045.
(45) Chen, Y.; Yan, W.; Guo, D.; Li, Y.; Li, J.; Liu, H.; Wei, L.; Yu, N.; Wang, B.; Zheng, Y.; Jing, M.; Zhao, J.; Ye, Y. An Activity-Based Sensing Fluorogenic Probe for Monitoring Ethylene in Living Cells and Plants. *Angew. Chem. Int. Ed.* **2021**, *60* (40), 21934–21942. https://doi.org/10.1002/anie.202108335.
(46) Kim, J.-H.; Shiratori, S. Fabrication of Color Changeable Film to Detect Ethylene Gas. *Jpn. J. Appl. Phys.* **2006**, *45* (5A), 4274–4278. https://doi.org/10.1143/jjap.45.4274.
(47) Cabanillas-Galan, P.; Farmer, L.; Hagan, T.; Nieuwenhuyzen, M.; James, S. L.; Lagunas, M. C. A new approach for the detection of ethylene using silica-supported palladium complexes. *Inorg. Chem.* **2008**, *47* (19), 9035–9041.
(48) Fong, D.; Luo, S.-X.; Andre, R. S.; Swager, T. M. Trace Ethylene Sensing via Wacker Oxidation. *ACS Central Science* **2020**, *6* (4), 507–512. https://doi.org/10.1021/acscentsci.0c00022.
(49) Hejl, A.; Day, M. W.; Grubbs, R. H. Latent Olefin Metathesis Catalysts Featuring Chelating Alkylidenes. *Organometallics* **2006**, *25* (26), 6149–6154. https://doi.org/10.1021/om060620u.
(50) Kost, T.; Sigalov, M.; Goldberg, I.; Ben-Asuly, A.; Lemcoff, N. G. Latent Sulfur Chelated Ruthenium Catalysts: Steric Acceleration Effects on Olefin Metathesis. *Journal of Organometallic Chemistry* **2008**, *693* (12), 2200–2203. https://doi.org/10.1016/j.jorganchem.2008.03.028.
(51) Monsaert, S.; Vila, A. L.; Drozdzak, R.; Voort, P. V. D.; Verpoort, F. Latent Olefin Metathesis Catalysts. *Chem. Soc. Rev.* **2009**, *38* (12), 3360–3372. https://doi.org/10.1039/B902345N.
(52) Nechmad, N. B.; Kobernik, V.; Tarannam, N.; Phatake, R.; Eivgi, O.; Kozuch, S.; Lemcoff, N. G. Reactivity and Selectivity in Ruthenium Sulfur-Chelated Diiodo Catalysts. *Angewandte Chemie International Edition* **2021**, *60* (12), 6372–6376. https://doi.org/10.1002/anie.202014929.
(53) Mori, M.; Sakakibara, N.; Kinoshita, A. Remarkable Effect of Ethylene Gas in the Intramolecular Enyne Metathesis of Terminal Alkynes. *J. Org. Chem.* **1998**, *63* (18), 6082–6083. https://doi.org/10.1021/jo980896e.
(54) Lloyd-Jones, G. C.; Margue, R. G.; de Vries, J. G. Rate Enhancement by Ethylene in the Ru-Catalyzed Ring-Closing Metathesis of Enynes: Evidence for an "Ene-Then-Yne" Pathway That Diverts through a Second Catalytic Cycle. *Angewandte Chemie International Edition* **2005**, *44* (45), 7442–7447. https://doi.org/10.1002/anie.200502243.
(55) Grotevendt, A. G. D.; Lummiss, J. A. M.; Mastronardi, M. L.; Fogg, D. E. Ethylene-Promoted versus Ethylene-Free Enyne Metathesis. *J. Am. Chem. Soc.* **2011**, *133* (40), 15918–15921. https://doi.org/10.1021/ja207388v.
(56) Hoveyda, A. H.; Liu, Z.; Qin, C.; Koengeter, T.; Mu, Y. Impact of Ethylene on Efficiency and Stereocontrol in Olefin Metathesis: When to Add It, When to Remove It, and When to Avoid It. *Angew. Chem. Int. Ed.* **2020**, *59* (50), 22324–22348. https://doi.org/10.1002/anie.202010205.
(57) Nechmad, N. B.; Phatake, R.; Ivry, E.; Poater, A.; Lemcoff, N. G. Unprecedented Selectivity of Ruthenium Iodide Benzylidenes in Olefin Metathesis Reactions. *Angew. Chem. Int. Ed.* **2020**, *59* (9), 3539–3543. https://doi.org/10.1002/anie.201914667.
(58) Blanco, C. O.; Sims, J.; Nascimento, D. L.; Goudreault, A. Y.; Steinmann, S. N.; Michel, C.; Fogg, D. E. The Impact of Water on Ru-Catalyzed Olefin Metathesis: Potent Deactivating Effects Even at Low Water Concentrations. *ACS Catalysis* **2021**, *11* (2), 893–899. https://doi.org/10.1021/acscatal.0c04279.
(59) Blanco, C. O.; Nascimento, D. L.; Fogg, D. E. Routes to High-Performing Ruthenium–Iodide Catalysts for Olefin Metathesis: Ligand Lability Is Key to Efficient Halide Exchange. *Organometallics* **2021**, *40* (12), 1811–1816. https://doi.org/10.1021/acs.organomet.1c00253.
(60) Nasibullin, I.; Yoshioka, H.; Mukaimine, A.; Nakamura, A.; Kusakari, Y.; Chang, T.-C.; Tanaka, K. Catalytic Olefin Metathesis in Blood. *Chem. Sci.* **2023**, *14* (40), 11033–11039. https://doi.org/10.1039/D3SC03785A.

(61) Tracz, A.; Matczak, M.; Urbaniak, K.; Skowerski, K. Nitro-Grela-Type Complexes Containing Iodides – Robust and Selective Catalysts for Olefin Metathesis under Challenging Conditions. *Beilstein J. Org. Chem.* **2015**, *11*, 1823–1832. https://doi.org/10.3762/bjoc.11.198.
(62) Blackmond, D. G. An Examination of the Role of Autocatalytic Cycles in the Chemistry of Proposed Primordial Reactions. *Angewandte Chemie International Edition* **2009**, *48* (2), 386–390. https://doi.org/10.1002/anie.200804565.
(63) Bissette, A. J.; Fletcher, S. P. Mechanisms of Autocatalysis. *Angewandte Chemie International Edition* **2013**, *52* (49), 12800–12826. https://doi.org/10.1002/anie.201303822.
(64) Hanopolskyi, A. I.; Smaliak, V. A.; Novichkov, A. I.; Semenov, S. N. Autocatalysis: Kinetics, Mechanisms and Design. *ChemSystemsChem* **2021**, *3* (1), e2000026. https://doi.org/10.1002/syst.202000026.
(65) Reuter, R.; Ward, T. R. Profluorescent Substrates for the Screening of Olefin Metathesis Catalysts. *Beilstein J. Org. Chem.* **2015**, *11* (1), 1886–1892. https://doi.org/10.3762/bjoc.11.203.
(66) Kajetanowicz, A.; Chatterjee, A.; Reuter, R.; Ward, T. R. Biotinylated Metathesis Catalysts: Synthesis and Performance in Ring Closing Metathesis. *Catal Lett* **2014**, *144* (3), 373–379. https://doi.org/10.1007/s10562-013-1179-z.
(67) Sun, X.; Li, Y.; He, W.; Ji, C.; Xia, P.; Wang, Y.; Du, S.; Li, H.; Raikhel, N.; Xiao, J.; Guo, H. Pyrazinamide and Derivatives Block Ethylene Biosynthesis by Inhibiting ACC Oxidase. *Nat. Commun.* **2017**, *8*. https://doi.org/10.1038/ncomms15758.
(68) Lieberman, M.; Hochstein, P. Ethylene Formation in Rat Liver Microsomes. *Science* **1966**, *152* (3719), 213. https://doi.org/10.1126/science.152.3719.213.
(69) Törnqvist, M.; Gustafsson, B.; Kautiainen, A.; Harms-Ringdahl, M.; Granath, F.; Ehrenberg, L. Unsaturated Lipids and Intestinal Bacteria as Sources of Endogenous Production of Ethene and Ethylene Oxide. *Carcinogenesis* **1989**, *10* (1), 39–41. https://doi.org/10.1093/carcin/10.1.39.
(70) Yang, W. S.; Stockwell, B. R. Ferroptosis: Death by Lipid Peroxidation. *Trends in Cell Biology* **2016**, *26* (3), 165–176. https://doi.org/10.1016/j.tcb.2015.10.014.
(71) Li, J.; Cao, F.; Yin, H.; Huang, Z.; Lin, Z.; Mao, N.; Sun, B.; Wang, G. Ferroptosis: Past, Present and Future. *Cell Death Dis* **2020**, *11* (2), 1–13. https://doi.org/10.1038/s41419-020-2298-2.